JP1.3

THE NUMERICAL EXPERIMENT OF THE ENERGY AND CO_2 IMBALANCE PROBLEM USING LES

Atsushi Inagaki*, Gerald Steinfeld **, Siegfried Raasch** and Manabu Kanda*
* Tokyo Institute of Technology, Tokyo, Japan
** University of Hannover, Hannover, Germany

1. INTRODUCTION

Recent studies have shown evidence of the non-closure of the energy balance when it is estimated using the eddy covariance (EC) method (e.g. Lee and Black, 1993). It is so-called energy imbalance problem. Sometimes the CO_2 flux is measured simultaneously with the sensible heat flux in a same EC system therefore the energy imbalance is thought to be associated with the CO_2 imbalance. There are few studies on the CO_2 imbalance problem in comparison with that on the energy imbalance so that the existence of the CO_2 imbalance is still under discussion. We evaluated the problem in a numerical simulation using the large-eddy simulation (LES) model, this numerical approach is following the study of the Kanda et al.(2004) or Inagaki (2005).

Some studies examined the analogy between the energy imbalance and the CO_2 imbalance in field experiments. Twine et al. (2000) examined the analogy based on the dependency of the imbalance on the friction velocity. Generally it is expected that the analogy between heat and CO_2 transport processes works better when the horizontal pattern of the surface heat and CO_2 flux are equivalently homogeneous, and it becomes getting worse when those horizontal pattern disagree. The present numerical study investigated the CO_2 imbalance in the following two situations; (1) ground surface heating and CO_2 sink are horizontally homogeneous, (2) surface heating is heterogeneous although the CO_2 sink is homogeneous.

2. THEORETICAL BACKGROUND

The current numerical study assumes the daytime convective boundary layer (CBL). All grids on a experimental surface (100m above the ground) in the domain are assumed to be EC measurement stations, where the EC flux and the imbalance of heat and CO_2 are calculated as following definition (Kanda et al., 2004);

$$I = (\overline{w'\phi'} - [\overline{F}])/[\overline{F}] \quad (1)$$

* *Corresponding author address*: Atsushi Inagaki, Tokyo Institute of Technology, Dept. of International Development Engineering, Meguro-ku, O-okayama, 2-12-1 Tokyo, 152-8552 JAPAN; e-mail: inagaki@ide.titech.ac.jp

where F is the kinetic flux, w is vertical velocity, ϕ is scalar (i. e. temperature and CO_2 concentration). The brackets $[\ ]$ expresses the spatial average, the over bar $\overline{\ }$ is temporal average, the superscript $'$ means the fluctuation from the temporal average. $\overline{w'\phi'}$ is the EC flux in a single grid.

Kanda et al. (2004) revealed that the domain average of the imbalance coincides with the temporal mean vertical advection $[\overline{w}\overline{\phi}]$.

$$[I] = -[\overline{w}\overline{\phi}]/[\overline{F}] \quad (2)$$

3. EXPERIMENTAL DESIGN

PALM (PArallelized Large eddy simulation Model) is a LES model developed by Raasch and Schröter (2001). PALM solves the Navier-Stokes equations for a Boussinesq fluid, the first law of thermodynamics and the equation for turbulent kinetic energy (TKE). Then CO_2 behaves as passive scalar. Subgrid-scale (SGS) turbulence is parameterized according to Deardorff (1980) with minor change. Non-divergence is assured at every time step by solving a Poisson equation for pressure. Cyclic conditions apply at the lateral boundaries. Monin-Obukhov similarity is assumed in the Prandtl layer between the ground surface and the first computational grid level. The roughness length is constant (0.1 m). Gravity waves are damped out from 1,800 m above the ground level.

The domain size is 16 x 16 x 2.7 km, grid spacing is 50 m for each direction. The initial temperature profile is set 0.8 K km^{-1} up to a height of 1,200 m and 7.4 K km^{-1} aloft for a strong capping inversion, which assumes a typical daytime ABL. CO_2 profile is initially constant (650 mg m^{-3}). Negative CO_2 flux (sink) is supplied from the ground horizontally homogeneously. The surface heat flux has horizontal variation as determined by the following equation,

$$F_{gv} = F_g + F_g A \sin\left(\frac{2\pi}{\lambda} x\right) \quad (3)$$

where F_{gv} is the ground surface heat flux at location x in the x-direction (K m s^{-1}). λ is wavelength (m), A is relative amplitude (%) of surface perturbation which becomes zero in the homogeneously heating

Table 1 Statistics in the homogeneously heating cases

Scalar	U_g (m s^{-1})	$[\overline{F}]$ (g m^{-2}s^{-1}) (K m s^{-1})	$[I]$ (%)	$[F_{SGS}]$ (%)
heat	0	0.0917	19.13	5.04
CO_2	0	-0.943	20.27	5.13
heat	4	0.0914	2.11	5.52
CO_2	4	-0.897	2.02	5.60

Ug: geostrophic wind, F_{SGS}: SGS contribution

cases. F_g is the mean heat flux over the ground level. In this study λ =8 km and F_g =0.1 K m s^{-1} were fixed in all simulations. The energy and CO_2 balances were analyzed at 100 m above the ground. The averaging time is 1 hour.

4. RESULTS

4.1 *Homogeneous surface heating case*

At first we address the cases of the horizontally homogeneous surface heat flux and CO_2 flux. Furthermore, we imposed geostrophic winds on the additional simulations to evaluate those dependencies on the energy or CO_2 imbalance.

Fig.1 shows the probability functions of the both kinds of imbalance which was measured at the all grids on the experimental surface. It is found that the analogy between the energy and CO_2 imbalance works very well. As termed in the previous section, the imbalance is caused by the temporal mean vertical advection. Fig.2 depicts the horizontal structure of the temporal mean vertical velocity, temperature and CO_2 concentration on the same xy-plane. The horizontal structures of the scalars are mostly same although the negative or positive signs are different (it depends the CO_2 sink or source condition). It is because the both scalars are transported by the same turbulent organized structure (TOS) as represented by the temporal mean vertical velocity. Therefore, the fractions of the heat and CO_2 flux due to the temporal mean flow are mostly same.

The geostrophic wind modify those mean structure dramatically (not shown) and decrease the fraction of the imbalances as shown in Fig.1 and Table1. However, the probability functions of the both kinds of imbalance remain analogous. It is because the horizontal structures of mean temperature and CO_2 concentration still remains similar pattern in the condition of the geostrophic wind (not shown).

4.2 *Heterogeneous surface heating case*

Horizontally one-dimensional sinusoidal variation was imposed on the surface heat flux as Eq.(3) although the surface CO_2 flux (sink condition) is homogeneous. The main difference from the homogeneous heating case is the development of the thermally induced mesoscale circulation.

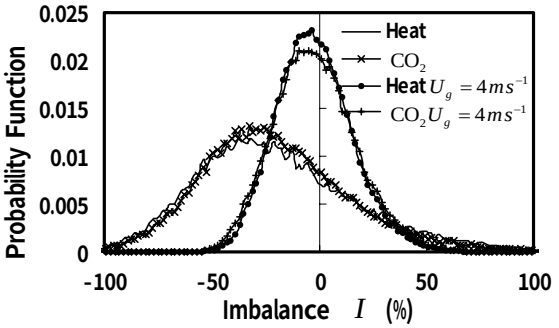

Fig. 1 Probability function of the energy and CO_2 imbalance (100m above the ground)

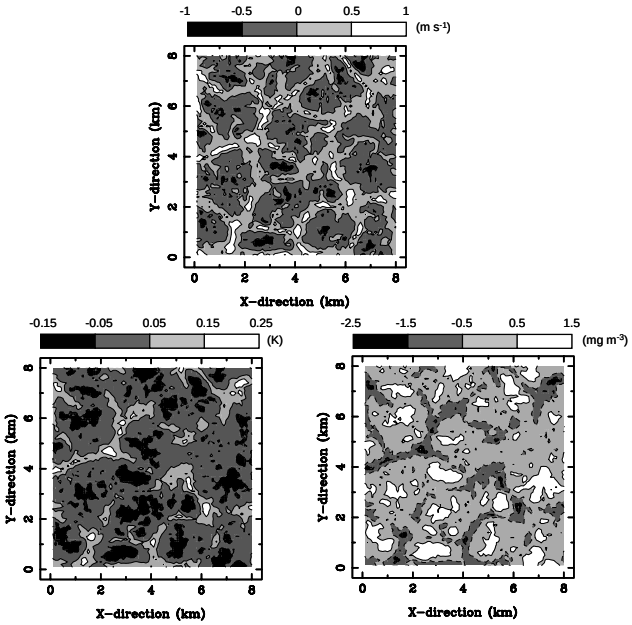

Fig.2 Horizontal structures of temporal mean variables
(top) vertical velocity,
(left) temperature, (right) CO_2 concentration

(a) Decomposition of advective flux

We decomposed the total vertical flux as follows,

$$[\overline{F}] = [\overline{w'\phi'}] + [[\overline{w}]_p[\overline{\phi}]_p] + F_{TOS}\,. \qquad (4)$$

where the first term on the right hand side is the domain average of the EC flux, the second term is the vertical flux due to the mesoscale circulation, the third term is the residual term, actually it is caused by the TOS (hereafter TOS flux).

The mesoscale circulation was represented by the phase average (Hadfield et al. 1995),

$$[\phi]_p(\hat{x}) = \frac{1}{N_p N_y}\sum_{y=1}^{Ny}\sum_{n=1}^{Np}\phi(\hat{x}+n\lambda, y) \qquad (5)$$

where $\hat{x} = x \bmod \lambda$ and $N_p = \dfrac{N_x dx}{\lambda}$

where the brackets $[\ ]_p$ indicate phase average.

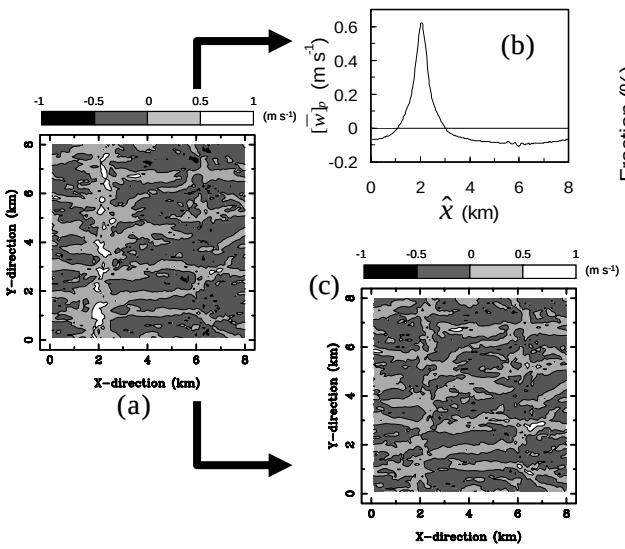

Fig.3 Mean vertical velocity structures
(a) temporal mean, (b) phase mean,
(c) TOS (temporal mean minus phase mean)

$\hat{x}$ is the new coordinate aligned with x, which represents the position in relation to a wave cycle of surface perturbation (such that the surface heating at $\hat{x} = \lambda / 4$ is maximum and $\hat{x} = 3\lambda / 4$ is a minimum), N_x, N_y and N_p are the total number of x- and y-grids, and the waves in the x-direction respectively, dx is the grid spacing in the x-direction.

By comparing Eq.(4) with Eq.(1), the imbalance is decompose into as follows (Inagaki et al. 2005),

$$-[I] = [\overline{w}\overline{\phi}] = [[\overline{w}]_p[\overline{\phi}]_p] + [F_{TOS}] \quad (6)$$

The sum of the mesoscale flux and the TOS flu x coincides with the imbalance.

(b) Decomposition of flow structure

As well as the flux decomposition described in Eq.(6), the horizontal pattern of the vertical advection is also decomposed into the mesoscale circulation and TOS. The phase average of the mean vertical velocity reduces to the mesoscale circulation $[\overline{w}]_p$ (Fig 2b). The maximum vertical velocity occurs at surface heating maxima ($\hat{x} = 2$km) and the minimum value at the surface heating minima ($\hat{x} = 6$km). As the TOS flux is defined by subtracting the mesoscale flux from the energy imbalance in Eq.(6), its corresponding flow structure is also represented by subtracting the one-dimensional mesoscale circulation (Fig.3b) from the two-dimensional pattern of the temporal mean vertical velocity (Fig.3a). Then the temporal mean TOS is extracted as shown in Fig. 3c. The TOS is a cluster of thermals moving with a larger time scale than that of individual plumes so that it still remained after the temporal average.

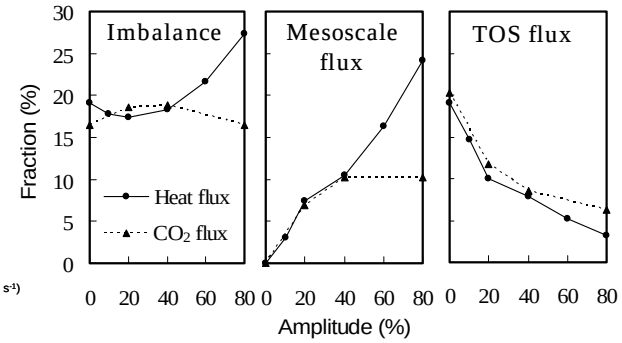

Fig.4 Domain-average of advective fluxes

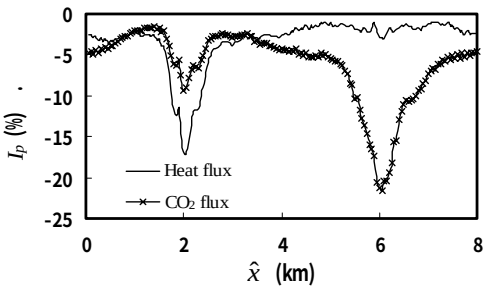

Fig.5 Phase-average of TOS flux

(c) Dependency on surface heating amplitude

Fig.4 shows the domain average of the advective fluxes shown in Eq.(6) for different surface heating amplitude. The mesoscale heat flux becomes larger than the mesoscale CO_2 flux when the surface heating amplitude is large. It is because the heterogeneity of surface heating is correlated to the mesoscale circulation compared to the horizontally homogeneous CO_2 sink pattern. Thus the heat is more efficiently transported by mesoscale circulation.

The other hands, the domain average of the TOS flux of CO_2 is similar to that of heat independent of the surface heating amplitude. We examined it more precisely.

(d) Phase average of the TOS flux

To address the local value of the TOS flux in phase, we examined the following scalar balance equation in phase.

$$[\overline{F}]_p = [\overline{w'\phi'}]_p + [\overline{w}]_p[\overline{\phi}]_p + [F_{TOS}]_p \quad (7)$$

Each term is according to those in Eq. (4) respectively. Fig.5 is the phase average of the TOS flux of heat and CO_2 (A=80%). The phase changes of the both kinds of TOS fluxes are different. The maximum peak of the TOS flux of heat occurred over the surface heating maxima, but that of CO_2 occurred over the minima.

Fig.6 shows the horizontal fluctuation of the temporal mean vertical velocity, temperature and CO_2 concentration along y-direction. The mesoscale circulation must be homogeneous along this direction so that this spatial fluctuation accounts for the TOS. Over the surface heating maxima, the vertical velocity and temperature distribution is more fluctuate than

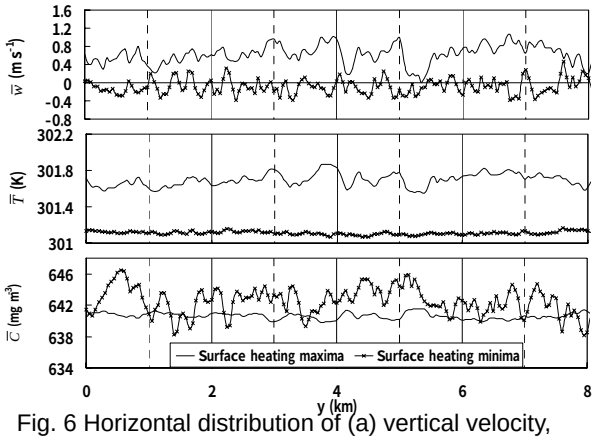

Fig. 6 Horizontal distribution of (a) vertical velocity, (b) temperature, and (c) CO_2 concentration, along y-direction

that over the surface heating minima because of the difference of the thermal activity. In contrast, the distribution of CO_2 concentration is more fluctuate over the surface heating minima than over the maxima. Therefore the TOS transported CO_2 efficiently over the surface heating minima.

To think the above, we show the vertical profiles of the temperature and CO_2 concentration over surface heating maxima and minima (Fig.7). If focusing on the experimental height (100m), the temperature becomes high over the heating maxima. The CO_2 concentration over the heating maxima and minima are comparable even though the mesoscale circulation carry the poor CO_2 air aloft over the heating minima and relatively high CO_2 air downward over the heating minima.

Over the surface heating minima, the downdraft of the mesoscale circulation suppress the development of the mixing height of the bottom air, therefore the poor CO_2 air near ground is concentrated there. This air is carried aloft by the TOS developed over surface heating minima as depicted in Fig.3c. It resulted in large negative CO_2 flux.

4. CONCLUSION

We investigated the energy and CO_2 imbalance over the homogeneous or heterogeneous surface heating region, and resulted in the follows;

(1) In the condition of the homogeneous surface heating and homogeneous CO_2 sink, the analogy between the energy imbalance and the CO_2 imbalance is very well even if the geostrophic wind is imposed.

(2) In the condition of the heterogeneous surface heating and homogeneous CO_2 sink condition, mesoscale heat flux becomes larger than that of CO_2 flux. The TOS fluxes of heat and CO_2 are comparable, however, their local values are much different. The maximum of TOS flux of heat occurs over the surface heating maxima but that of CO_2 occurs over the heating minima. It is because the mesoscale downdraft suppressed the development of the mixing

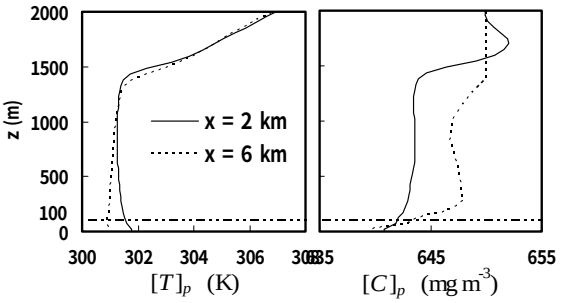

Fig. 7 Vertical profiles of temperature and CO_2 concentration over the surface heating maxima (x=2km) and minima (x=6km)

height over the surface heating minima where the bottom poor CO_2 air is much concentrated and is taken aloft by TOS.

ACKNOWLEDGEMENTS

This research was supported by CREST (Core Research for Evolution Science and Technology) of JST (Japan Science and Technology cooperation) and by a Grant-in-Aid for Developmental Science Research from the Ministry of Education, Science and Culture of Japan.

REFERENCES

Deardorff, J.W., 1980: Stratocumulus-topped mixed layers derived from a three-dimensional model, Boundary-Layer Meteorol., **18**, 495–527.

Hadfield, M.G., W.R. Cotton, and R.A. Pielke 1991: Large-Eddy Simulations of Thermally Forced Circulations in the Convective Boundary Layer. Part1: A Small-Scale Circulation with Zero Wind. *Boundary-Layer Meteorol*., **57**, 79-114.

Inagaki, A., Letzel, M.O., Raasch, S., Kanda, M., 2005: Impact of surface heterogeneity on energy imbalance: a study using LES, *J. Meteor. Soc. Japan*, submitted.

Kanda, M., Inagaki, A., Letzel, M.O., Raasch, S., Watanabe, T.,2004: Les study of the energy imbalance problem with eddy covariance fluxes, Boundary-Layer Meteorol., **110**, 381-404.

Lee, X. and Black, T. A., 1993: Atmospheric Turbulence within and above a Douglas-Fir Stand. Part2: Eddy Fluxes of Sensible Heat and Water Vapour, Boundary-Layer Meteorol., **64**, 369–389.

Raasch, S. and Schröter, M., 2001 : PALM - A large-eddy simulation model performing on massively parallel computers. Meteorol. Z., **10**, 363-372.

Twine, T.E., Kustas, W.P., Norman, J.M., Cook, D.R., Houser, P.R., Meyers, T.P., Prueger, J.H., Starks, P.J., Wesley, M.L., 2000: 'Correcting eddy-covariance flux underestimates over a grassland', *Agric.For.Meteorol.*, **103**, 279-300.